Supporting information

Regulating oxygen functionalities of cellulose-derived hard carbon toward superior sodium storage

Boyang Zhao[a], Xiaotian Li[a], Lei Shang[a], Chuang Qiu[a], Renlu Yuan[a], Haiyan Liu[b], Tao Liu[b], Ang Li[a], Xiaohong Chen[a], Huaihe Song[a]*

a. State Key Laboratory of Chemical Resource Engineering, Beijing Key Laboratory of Electrochemical Process and Technology, Beijing University of Chemical Technology, Beijing 100029, China

b. National Engineering Research Center of Coal Gasification and Coal-Based Advanced Materials, Shandong Energy Group CO, LTD, Jinan, China

**Corresponding author.*

Email addresses: songhh@mail.buct.edu.cn (H. Song)

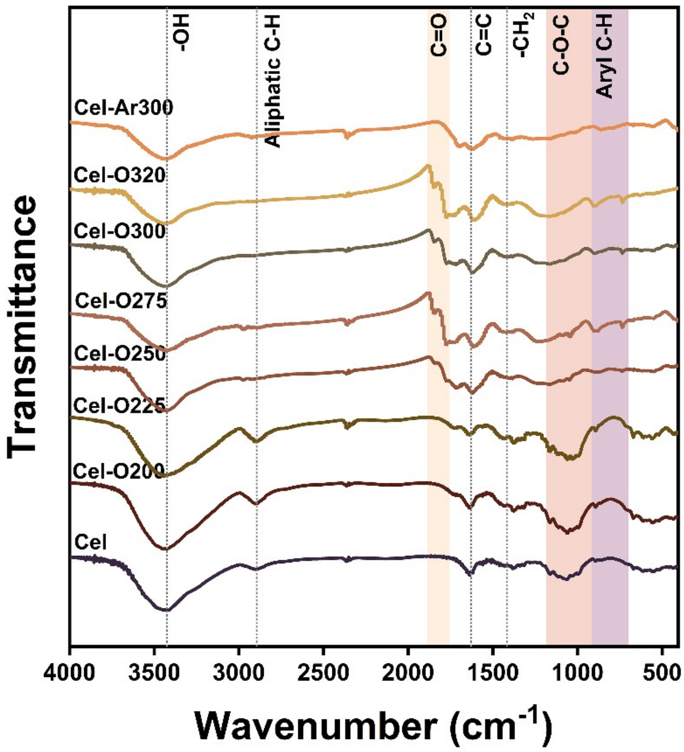

Fig. S1. FTIR spectra of Cel-Ox.

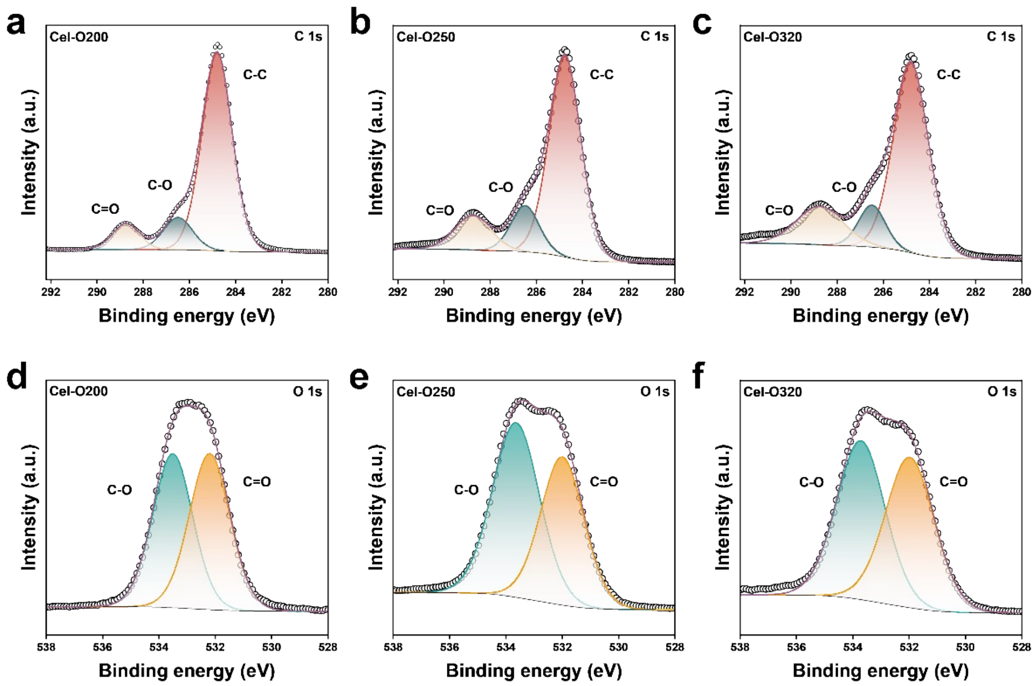

Fig. S2. High resolution C 1s and O 1s spectra of Cel-O200, Cel-O250, and Cel-O320.

Table S1. The content of the C 1s and O 1s peaks in Cel-Ox.

B.E. (eV)	C1 (284.80)	C2 (286.49)	C3 (284.75)	O1 (531.98)	O2 (533.51)
Assignment	C–C	C–O	C=O	C=O	C–O
Cel-O200	78.41	12.41	9.81	49.22	50.78
Cel-O250	71.55	14.53	13.92	56.11	43.89
Cel-O300	77.13	13.49	9.83	57.13	42.87
Cel-O320	69.45	11.75	18.80	51.13	48.87
Cel-Ar300	79.07	14.43	6.50	46.10	53.90

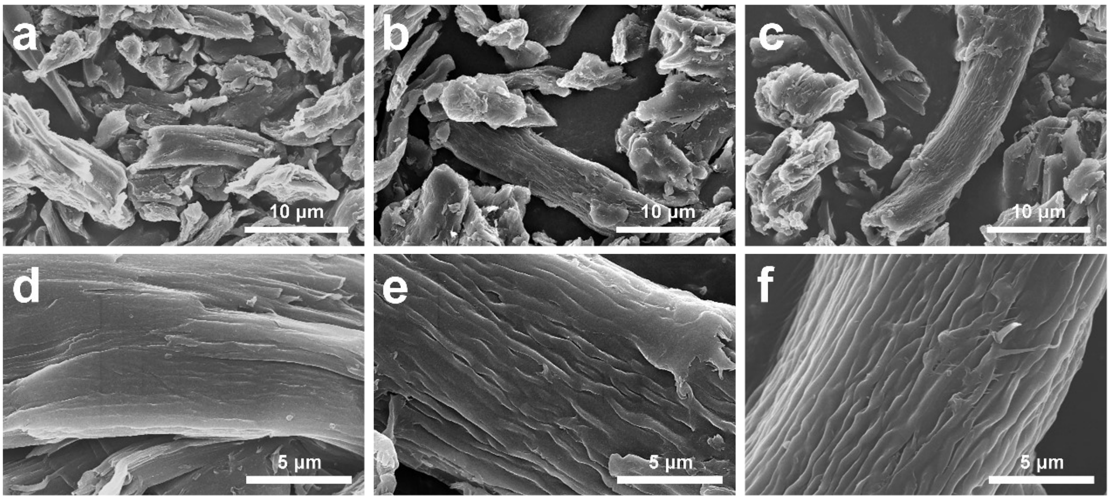

Fig. S3. SEM images of (a, d) Cel-O200-1500, (b, e) Cel-O250-1500, (c, f) Cel-O320-1500.

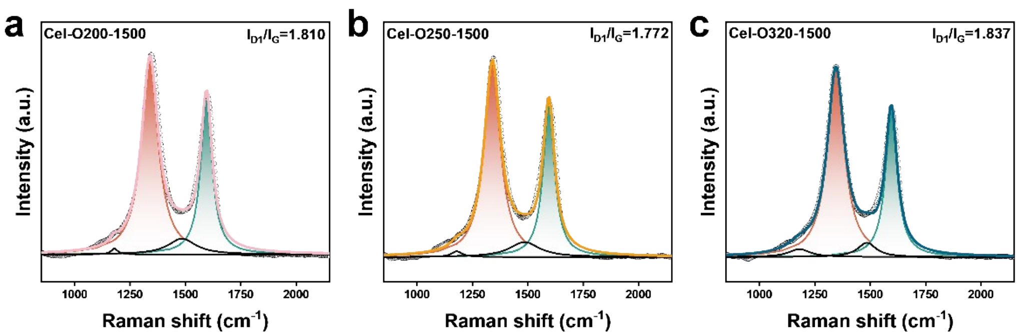

Fig. S4. Raman spectra of Cel-O200-1500, Cel-O250-1500, Cel-O320-1500.

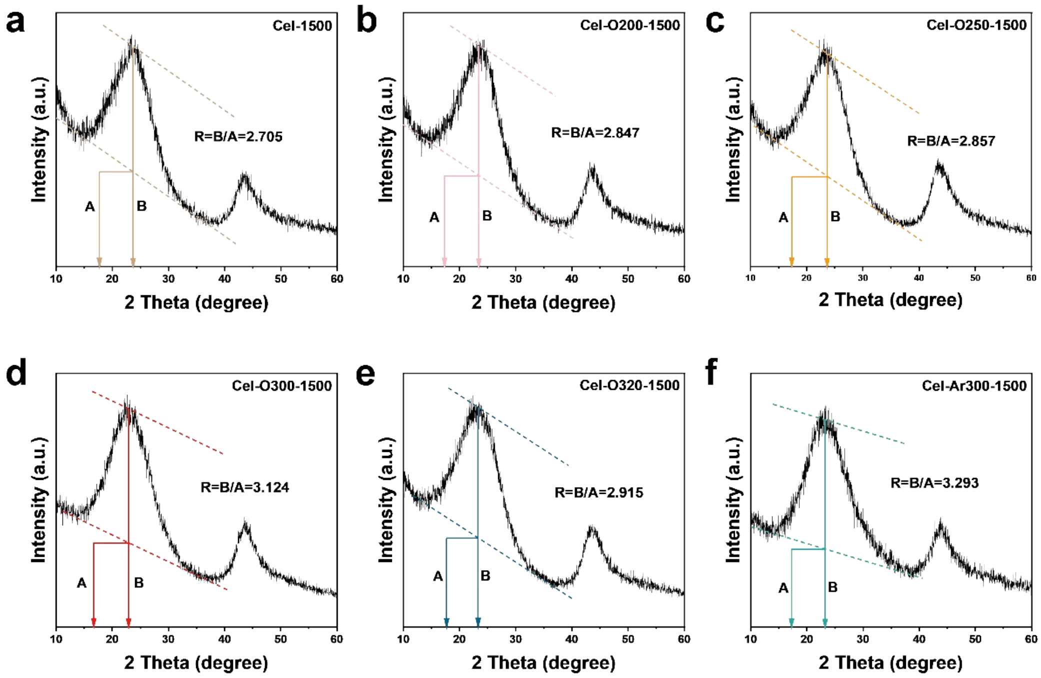

Fig. S5. Calculation of R values of Cel-1500, Cel-Ox-1500, and Cel-Ar300-1500.

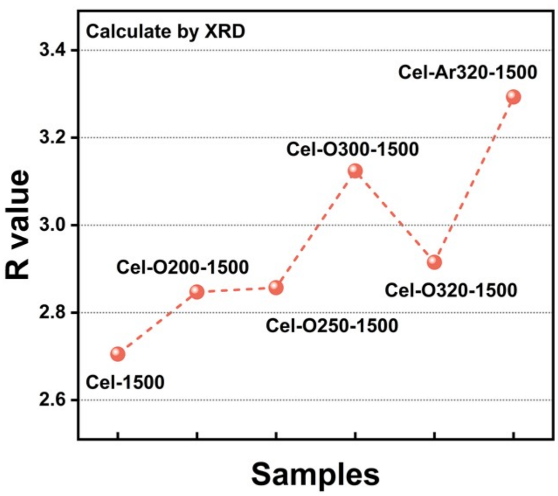

Fig. S6. The variation pattern of R values.

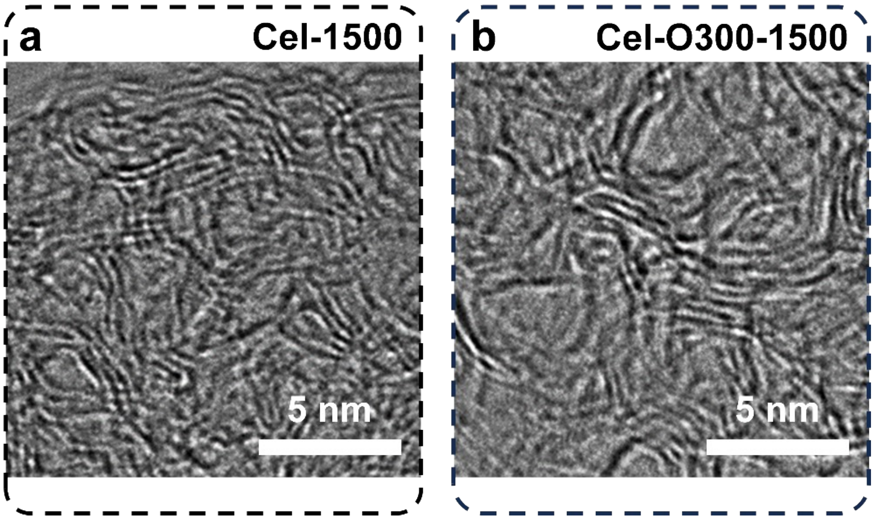

Fig. S7. HRTEM images of Cel-1500 and Cel-O300-1500.

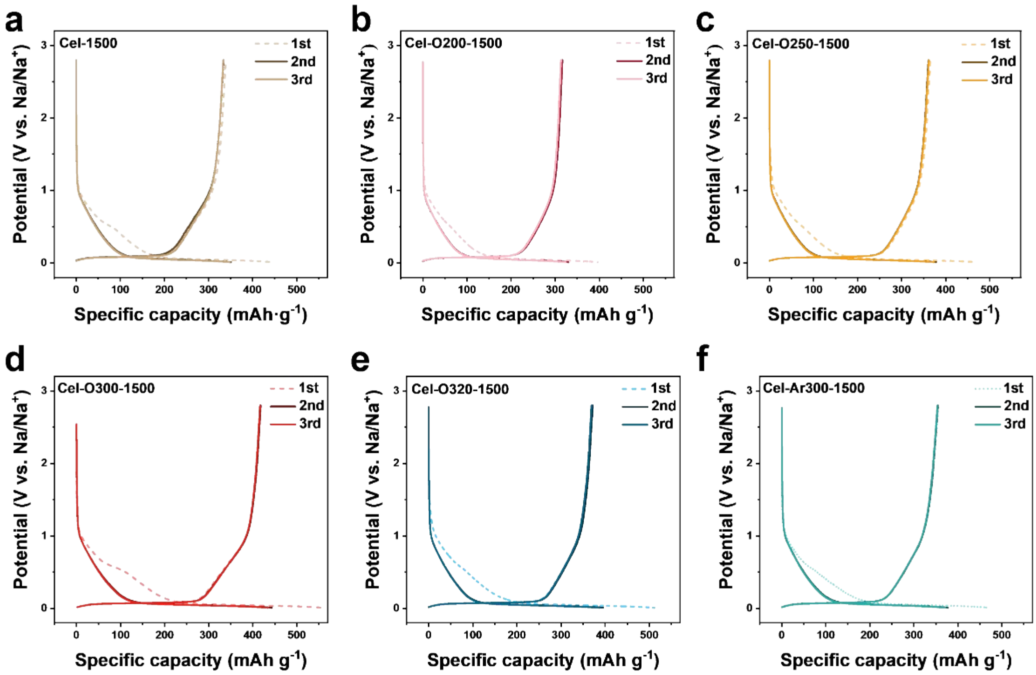

Fig. S8. GCD profiles of Cel-1500, Cel-Ox-1500 and Cel-Ar300-1500 during the initial three cycles.

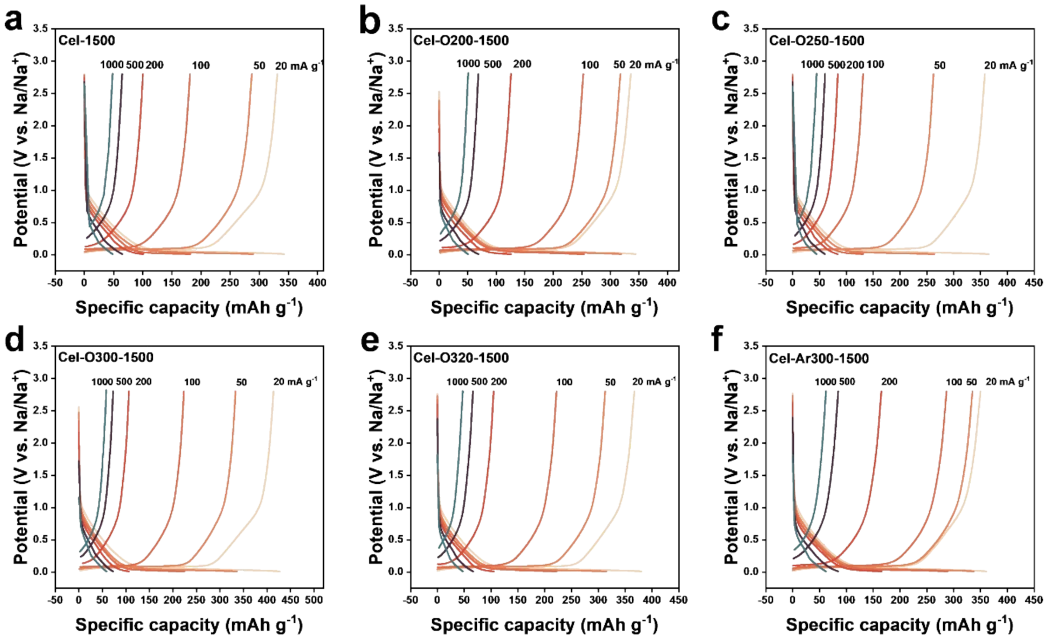

Fig. S9. GCD profiles of Cel-1500, Cel-Ox-1500 and Cel-Ar300-1500 at different current density in SIBs.

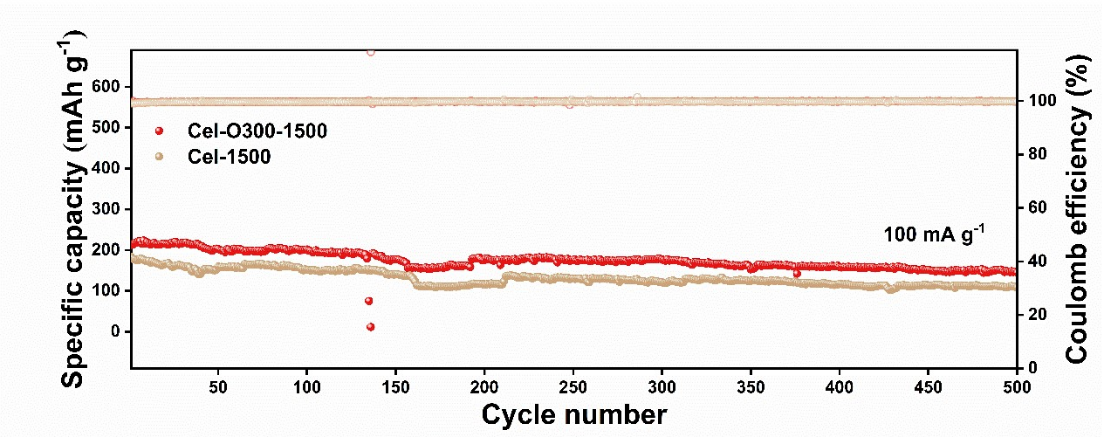

Fig. S10. long-term cycling performance and coulombic efficiency at 100 mA g^{-1} of Cel-O300-1500 and Cel-1500.

Table S2. The electrochemical performance and plateau capacity ratio of cellulose-derived hard carbon samples measured at 20 mA g^{-1}.

Samples	Reversible Capacity (mAh g^{-1})	ICE (%)	Plateau Capacity (mAh g^{-1})	The proportion of the Plateau capacity
Cel-1500	342.5	76.6	235.2	0.687
Cel-O200-1500	344.4	71.9	238.8	0.693
Cel-O250-1500	365.6	77.9	262.8	0.719
Cel-O300-1500	426.8	74.8	307.5	0.721
Cel-O320-1500	380.2	72.4	275.5	0.725
Cel-Ar300-1500	361.0	75.6	246.1	0.682

Table S3. Kinetic fitting parameters and calculated D according to EIS test.

Samples	Re (Ω)	Rf (Ω)	Rct (Ω)	σ (Ω $s^{-1/2}$)	D (cm^2 s^{-1})
Cel-1500	4.886	5.824	76.81	933.33	3.18478E-12
Cel-Ar300-1500	6.102	4.831	33.44	782.91	4.52612E-12
Cel-O300-1500	4.836	2.143	41.07	1135.99	2.14982E-12

Table S4. Summary of reported pre-oxidation-related and cellulose-derived hard carbon anodes for SIBs.

Samples	Pyrolysis temperature (°C)	S_{BET} (m^2 g^{-1})	d (002) (nm)	Reversible capacity (mAh g^{-1})	ICE (%)	Ref.
Phenolic Resin (PFHC-20)	1100	35.3	0.389	334.3 (20 mA g^{-1})	84.7	[1]
Bituminous coal (RC-GO-1200)	1200	8.4	0.380	274.2 (30 mA g^{-1})	74.8	[2]

Esterified starch (H300-1100)	1100	2.9	0.387	369.8 (20 mA g^{-1})	82.5	3
D-glucose powder (G-220-1300)	1300	6.0	0.364	308.0 (25 mA g^{-1})	84.0	4
Asphalt (HC-325-9)	1100	367.9	0.389	286.9 (10 mA g^{-1})	83.6	5
Cotton	1300	38.0	0.410	260.0 (20 mA g^{-1})	72.0	6
Cellulose nanofibers	1000	377.0	—	255.0 (40 mA g^{-1})	58.8	7
Microcrystalline cellulose	1600	<10	0.376	310.0 (37.2 mA g^{-1})	84.0	8
Filter paper (DPC-A)	800	761.0	—	289.0 (20 mA g^{-1})	81.0	9
Nanocellulose (Spinifex derived)	1000	154.0	0.390	386.0 (20 mA g^{-1})	50.0	10
Cellulose nanocrystals (CNCs)	1000	145.6	0.390	340.0 (100 mA g^{-1})	—	11
Microcrystalline cellulose	1400	5.0	0.373	310.0 (37.2 mA g^{-1})	82.7	12
Cellulose powder derived from cotton linter	1300	506.0	0.389	351.0 (25 mA g^{-1})	68.0	13
Filter Paper (MV-HC)	1100	379.0	—	308.0 (20 mA g^{-1})	68.0	14
Microcrystalline cellulose (BHC-CO_2)	1000	96.0	0.350	293.5 (50 mA g^{-1})	39.5	15
Nanocellulose powder	1200	—	—	250.0 (100 mA g^{-1})	—	16
Microcrystalline cellulose (HC-88.5)	1300	281.8	0.404	322.0 (50 mA g^{-1})	—	17
Microcrystalline cellulose (MCC-1400)	1400	5.8	0.388	343.3 (20 mA·g-1)	87.3	18
Cellulose fiber (HC-Cell)	1300	5.1	0.381	332.0 (0.2 C)	83.0	19
cellulose and lignin mixed at amass ratio of	1400	53.0	0.384	259.0 (100 mA g^{-1})	—	20

1:1 (CL-HC)						
bacterial cellulose (T-SBC-1300)	1300	51.2	0.390	239.0 (30 mA g^{-1})	56.9	[21]
α-cellulose (Cel-O300-1500)	1500	8.7	0.383	426.8 (20 mA g^{-1})	74.8	**This work**

Reference

1 G. Zhang, L. Zhang, Q. Ren, L. Yan, F. Zhang, W. Lv and Z. Shi, *ACS Appl. Mater. Interfaces*, 2021, **13**, 31650–31659.

2 Z. Lou, H. Wang, D. Wu, F. Sun, J. Gao, X. Lai and G. Zhao, *Fuel*, 2022, **310**, 122072.

3 M. Song, Z. Yi, R. Xu, J. Chen, J. Cheng, Z. Wang, Q. Liu, Q. Guo, L. Xie and C. Chen, *Energy Storage Materials*, 2022, **51**, 620–629.

4 Z. V. Bobyleva, O. A. Drozhzhin, A. M. Alekseeva, K. A. Dosaev, G. S. Peters, G. P. Lakienko, T. I. Perfilyeva, N. A. Sobolev, K. I. Maslakov, S. V. Savilov, A. M. Abakumov and E. V. Antipov, *ACS Appl. Energy Mater.*, 2023, **6**, 181–190.

5 R. Xu, Z. Yi, M. Song, J. Chen, X. Wei, F. Su, L. Dai, G. Sun, F. Yang, L. Xie and C.-M. Chen, *Carbon*, 2023, **206**, 94–104.

6 Y. Li, Y.-S. Hu, M.-M. Titirici, L. Chen and X. Huang, *Adv. Energy Mater.*, 2016, **6**, 1600659.

7 W. Luo, J. Schardt, C. Bommier, B. Wang, J. Razink, J. Simonsen and X. Ji, *J. Mater. Chem. A*, 2013, **1**, 10662.

8 V. Simone, A. Boulineau, A. de Geyer, D. Rouchon, L. Simonin and S. Martinet, *Journal of Energy Chemistry*, 2016, **25**, 761–768.

9 P. Zheng, T. Liu and S. Guo, *Sci Rep*, 2016, **6**, 35620.

10 R. R. Gaddam, E. Jiang, N. Amiralian, P. K. Annamalai, D. J. Martin, N. A. Kumar and X. S. Zhao, *Sustainable Energy Fuels*, 2017, **1**, 1090–1097.

11 H. Zhu, F. Shen, W. Luo, S. Zhu, M. Zhao, B. Natarajan, J. Dai, L. Zhou, X. Ji, R. S. Yassar, T. Li and L. Hu, *Nano Energy*, 2017, **33**, 37–44.

12 C. M. Ghimbeu, *Nano Energy*.

13 H. Yamamoto, S. Muratsubaki, K. Kubota, M. Fukunishi, H. Watanabe, J. Kim and S. Komaba, *J. Mater. Chem. A*, 2018, **6**, 16844–16848.

14 Z. Li, Y. Chen, Z. Jian, H. Jiang, J. J. Razink, W. F. Stickle, J. C. Neuefeind and X. Ji, *Chem. Mater.*, 2018, **30**, 4536–4542.

15 H. Wang, F. Sun, Z. Qu, K. Wang, L. Wang, X. Pi, J. Gao and G. Zhao, *ACS Sustainable Chem. Eng.*, 2019, **7**, 18554–18565.

16 L. Li, D. Chen, S. Su and B. Zeng, *mat express*, 2020, **10**, 1685–1691.

17 S. Alvin, C. Chandra and J. Kim, *Chemical Engineering Journal*, 2021, **411**, 128490.

18 X.-S. Wu, X.-L. Dong, B.-Y. Wang, J.-L. Xia and W.-C. Li, *Renewable Energy*, 2022, **189**, 630–638.

19 J. Conder, C. Villevieille, J.-M. Le Meins and C. Matei Ghimbeu, *ACS Appl. Energy Mater.*, 2022, **5**, 12373–12387.

20 Q. Jin, L. Tao, Y. Feng, D. Xia, G. A. Spiering, A. Hu, R. Moore, F. Lin and H. Huang, *ACS Sustainable Chem. Eng.*, 2023, **11**, 536–546.

21 F. Wang, T. Zhang and F. Ran, *Electrochimica Acta*, 2023, **441**, 141770.